Nordic Hydrology, 16, 1985, 203-212

Application Limits for the Kinematic Wave Approximation

Willi H. Hager
École Polytechnique Fédérale de Lausanne,
CH-1015, Lausanne, Switzerland

Kurt Hager
Kuster & Hager, CH-8730 Uznach, Switzerland

Flows with *predominate* flow direction are governed by the de Saint Venant flow equations. The kinematic wave approach retains the mass balance but considers pseudo-uniform flow conditions instead of the full momentum balance. This approximation is particularly well-suited for overland runoff processes. The zero-inertia approach may be regarded as an intermediate formulation which retains the effect of surface slope but neglects dynamical flow properties. This investigation considers in detail the differences between the three of the aforementioned approaches under pseudo-steady flow conditions. The result indicates application limits of the two simplified wave theories when compared to the de Saint Venant flow equations and may be regarded as a useful decisive criterion.

Introduction

The hydrological modelling of overland and stream runoff in a watershed is either based on the hydrodynamic flow equations, or the main runoff features are modelled by a simplified, semi-empirical approach. Although the first approach will steadily replace the second because of its methodology, a full description of the flow processes is far from being simple. As an example, the turbulence characteristics of these flows are usually accounted for empirically such as by the Manning formula. Furthermore, effects of surface tension for overland flow and effects of streamline curvature for streamflow are ignored.

These facts have led hydrologists to consider less sophisticated approaches. Evi-

dently, effects of streamline curvature may be ignored for overland flow since the assumptions governing the shallow water flow theory are ideally fulfilled. Also it is sufficient to consider one-dimensional flow conditions for which transverse effects vanish. The governing equations then can be reduced to the generalised approach of de Saint Venant (Liggett 1975). This set of first order, non-linear partial differential equations (PDE) can further be simplified for overland flow by considering the cross-sectional area as wide rectangle. Yet, the numerical solution procedure is far from being elementary, since stability and convergence criteria must be respected. Furthermore, any spatial or temporal abrupt change of a basic parameter such as the bottom slope, the excess precipitation intensity or the roughness characteristics may develop *shock waves* which must be modelled properly. This latter peculiarity is typical for the hyperbolic character of the governing PDE and is discussed in detail by Borah et al (1980).

In order to adopt a middle course between the poorly defined, basic model specifications (such as the excess rainfall, the surface roughness characteristics, among others) and the aforementioned governing equations, hydrologists have tried to simplify the de Saint Venant flow equations. Some of the often used simplifications are discussed in detail by Woolhiser (1975). In practice, the *zero-inertia* and the *kinematic wave approach* have become particularly important. The resulting system of PDE then accounts for the complete continuity relation but adopts simpler versions of the dynamical flow equation (see later Eqs. (10)-(11)). The full description according to de Saint Venant takes *dynamical* waves into consideration, while the zero-inertia approach corresponds to a set of parabolic PDE (Raudkivi 1979), thereby accounting for *diffusive* flow effects. Finally, the kinematic wave approximation is again of hyperbolic nature but may be expressed as a first order PDE for either flow depth or discharge. The propagation velocity is variable, but there are no diffusive effects (a wave crest in a uniform channel is not damped, therefore).

The first systematic investigation of the three aforementioned approaches is provided by Lighthill and Whitham (1955). The formation of shock waves in the dynamic and kinematic wave approaches is described in detail.

Weinmann and Laurenson (1979) compare various one-dimensional approaches (including the aforementioned) for typical flow situations in open channel flow. Woolhiser and Liggett (1967) find that the kinematic wave approximation yields results comparable to these determined by the more general approaches provided a typical Froude number, $\mathbf{F}_o$, is always below 2 and the *kinematic wave number* $k=S_oL/(h_o\mathbf{F}_o^2)>10$ in which S_o, L, h_o are typical bottom slope, length and flow depth, respectively. k may be interpreted as the product of the ratio of the typical elevation difference (S_oL) between lowest and highest points of a reach and flow depth times the inverse Froude number. The first term accounts for the *shallowness* of the flow, while the second, $\mathbf{F}_o$, reflects *dynamical* effects. The de Saint-Venant flow equations can be replaced by the kinematic wave approximation whenever

$k>10$ without loss of substantial accuracy. However, the criterion $k>10$ is not readily applicable since h_o and $\mathbf{F}_o$ are a priori unknown. The purpose of the present investigation is to overcome this lack and provide *direct* application criteria for the kinematic wave approximation. In order to have a feasible approach, quasi-steady flow conditions as occur in the vicinity for temporal maximum excess precipitation are investigated. This is in agreement with k as defined previously, in which no time-dependent quantity appears.

Governing Equations

Consider steady, one-dimensional flow on a plane of constant bottom slope, S_o, on which flow depth, h, is much smaller than the width. The discharge per unit width, q, then is given by

$$q = Vh \tag{1}$$

in which V is average velocity. The momentum balance in longitudinal direction may be expressed as (Hager 1983)

$$\frac{d}{dx}\left(\frac{h^2}{2}+\frac{q^2}{gh}\right) \equiv (S_0-S_f)h+\frac{u\cos\phi}{g}\frac{dq}{dx} \tag{2}$$

in which x is the longitudinal coordinate, g the gravitational acceleration, S_f the frictional slope, $u\cos\phi$ the streamwise velocity component of the lateral inflow or outflow intensity dq/dx, see Fig. 1. This may equally be expressed as

$$h' \equiv \frac{S_0-S_f+(q'/gh)(u\cos\phi-2V)}{1-F^2} \tag{3}$$

in which $\mathbf{F} = V/\sqrt{gh}$ is the Froude number. Eq. (3) corresponds to a particular case of the general flow equation as derived in (Liggett 1975), which accounts for the non-uniform velocity distribution and the non-uniform velocity distribution and the non-prismatic channel cross-section. The present approach is based on a uniform velocity and a hydrostatic pressure distribution. These are reasonable assumptions for *shallow* water flow phenomena as appear in overland flow (Woolhiser 1975).

Intensities of the lateral inflow, p_i, and the lateral outflow, p_o are assumed independent of the longitudinal coordinate, such that $p=p_i-p_o$ is independent of x.

Since $dq/dx=q'=p$, the local discharge distribution is

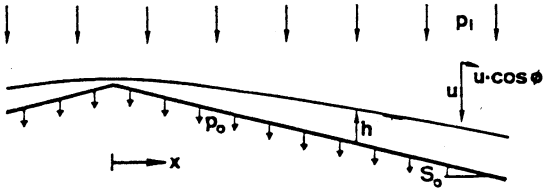

Fig. 1. Definition of flow pattern.

$$q = p\,x \tag{4}$$

in which $x=0$ corresponds to the upstream end of the reach, see Fig. 1. For small and moderate bottom slope, the streamwise lateral velocity component is much smaller than the channel velocity, $|u\cos\phi/V|\ll 1$. Eq. (3) then simplifies to

$$h' = \frac{S_0 - S_f - (2pq/gh^2)}{1 - F^2} \tag{5}$$

in which the local discharge distribution is given by Eq. (4). For *turbulent* flow conditions, the frictional slope is approximated with the Manning-Strickler formula

$$S_f = \frac{q^2}{K^2 h^{10/3}} \tag{6}$$

$K=1/n$ being the roughness coefficient and the hydraulic radius is equal to the flow depth h. Imposing one boundary condition then yields the free surface profile $h(x)$, which will be studied in more detail in the subsequent sections.

Approximations

The governing momentum Eq. (5) accounts for shallow water flow conditions, for which the ratio of a typical flow depth to a typical length scale vanishes. Whenever this condition is not fulfilled effects of the transverse velocity and pressure distributions must be accounted for, see e.g. (Hager and Hutter 1984). Let

$$\bar{x} = \frac{S_0 x}{h_0} \quad , \quad \bar{h} = \frac{h}{h_0} \quad , \quad \bar{V} = \frac{V}{V_0} \tag{7}$$

h_o and V_o being typical flow depth and velocity, respectively. Eq. (5) then transforms into

$$\frac{d\bar{h}}{d\bar{x}} = \frac{1 - (\chi \bar{V}^2/\bar{h}^{4/3}) - 2\rho F_0^2(\bar{V}/\bar{h})}{1 - F_0^2(\bar{V}^2/\bar{h})} \tag{8}$$

in which

$$\chi = \left(\frac{V_0}{K\sqrt{S_0}\, h_0^{2/3}}\right)^2 \quad , \quad \rho = \frac{p}{V_0 S_0} \quad , \quad F_0 = \frac{V_0}{\sqrt{g h_0}} \tag{9}$$

χ may be identified as the ratio between a typical velocity and the uniform flow velocity and accounts for frictional effects, while ϱ is the ratio between the precipitation velocity and the typical velocity times the bottom slope. Finally, $\mathbf{F}_o$ ist the typical Froude number.

It is a well-known fact that overland flow is usually *subcritical*, and typical Froude numbers are $0<\mathbf{F}_o<0.2$ for extreme excess precipitation as appears during

thunderstorms. Asymptotically, $\mathbf{F}_o \rightarrow 0$, for which Eq. (8) simplifies to $d\bar{h}/d\bar{x}=1-(\chi\bar{V}^2/\bar{h}^{1/3})$, corresponding to

$$\frac{dh}{dx} = S_0 - S_f \tag{10}$$

which is referred to as *zero-inertia* flow equation (Katopodes 1982). An even more drastic simplification of the above relation equates only the right hand side of Eq. (10), the result being the so-called *kinematic wave approximation*

$$S_0 - S_f = 0 \tag{11}$$

It is important to recognize that all of the three above approaches, namely Eqs. (5), (10) and (11), apply to particular flow configurations, and may yield nearly identical solutions under certain circumstances. However, the degree of liberty of Eqs. (5) and (10) is higher than for Eq. (11), since one boundary condition can be imposed. Because flow conditions for overland flow are globally subcritical, the boundary condition in question must be imposed at the *downstream* end of the considered reach. The resulting upstream flow depth then generally turns out to be different from $h=0$, while $h(q=0)=0$ according to Eq. (11). Purpose of ensuing considerations will be a more detailed investigation of this peculiarity and determination of *application criteria* for the kinematic wave theory with respect to the overland flow phenomena.

Non-Dimensional Formulation

Using Eqs. (4)-(6) the governing relation of the free surface profile is

$$h' \equiv \frac{S_0 - (p^2x^2/K^2h^{10/3}) - (2p^2x/gh^2)}{1 - (p^2x^2/gh^3)} \tag{12}$$

Distinction between sub- and supercritical flow conditions must be made. For $\mathbf{F}^2=p^2x^2/(gh^3)<1$, the direction of computation is reversed to the flow direction, while the two respective directions are identical for $\mathbf{F}>1$. Consequently the boundary condition must be imposed at the downstream end for $\mathbf{F}<1$, and at the upstream end for $\mathbf{F}>1$. However, no boundary condition is available at the two respective locations for a sufficiently long reach having constant, positive bottom slope from physical arguments. By inspecting the mathematical properties of Eq. (12) it is noted that the conditions

$$S_0 - \frac{p^2x_s^2}{K^2h_s^{10/3}} - \frac{2p^2x_s}{gh_s^2} = 0 \tag{13}$$

$$1 - \frac{p^2x_s^2}{gh_s^3} = 0 \tag{14}$$

define the *singular point* $x=x_s$ of Eq. (12). Further, it can be shown (Hager 1981 and 1983) that this point may be used as computational origin. Eliminating x_s between the two relations yields

$$S_0 - \frac{g}{K^2 h_s^{1/3}} - \frac{2p}{\sqrt{g h_s}} = 0 \qquad (15)$$

for h_s, and the loaction x_s of the critical point is given by Eq. (14). The coordinates (x_s,h_s) are influenced by the friction coefficient K, the bottom slope S_0 and the precipitation intensity p. These quantites will be used as scalings. However, this cannot be achieved with the expressions as given in Eq. (13). To this end, it is important to note that the last term is much smaller than S_0. A typical bottom slope is $S_0=0.1$, while p has the order $p=10\text{mm}/h=2.8\times10^{-6}$ m/s, and a typical flow depth (under this high excess precipitation) is $h=0.01$ m. The term in question then becomes $2p/\sqrt{gh}=1.8\times10^{-5}\ll S_0$. This property has also been described by Raudkivi (1979) among others, and it is common to neglect the longitudinal momentum component excerted by the lateral inflow. By letting

$$X = \frac{p(K\sqrt{S_0})^9 x}{g^5} \quad , \quad y = \frac{(K\sqrt{S_0})^6 h}{g^3} \qquad (16)$$

Eqs. (13) and (14) transform into

$$y^{10/3} - X^2 = 0 \quad , \quad y^3 - X^2 \equiv 0 \qquad (17)$$

and the governing equation of the surface profile is

$$y' = \frac{1}{\eta}\left(\frac{1-(X^2/y^{10/3})}{1-\delta(X^2/y^3)}\right) \qquad (18)$$

in which δ is an integer and

$$\eta = pK^3\sqrt{S_0}/g^2 \qquad (19)$$

A typical order of K is 10^1 ($m^{1/3}/s$), such that $\eta=0(10^{-5})$ if the above typical numbers for p and S_0 are used. The dynamical flow Eq. (12) is reproduced by letting $\eta>0$ and $\delta=1$, while the zero-inertia Eq. (10) is given by $\eta>0$ and $\delta=0$. Finally the kinematic wave approximation corresponds to $\eta=\delta=0$. The free surface slope at the singular point $(X_s,y_s)=(1,1)$ of Eq. (18), is computed using Hopital's rule; the result is

$$y_s' = \frac{1}{3\eta}\left(\eta + \frac{5}{3} \pm \sqrt{\frac{25}{9} - \frac{8}{3}\eta + \eta^2}\right) \qquad (20)$$

It can be demonstrated that the positive root sign corresponds to the transition **F** >1 to **F** <1 which is not considered here (hydraulic jump), while the negative root sign indicates flows with increasing Froude number. Eq. (20) with the negative root sign allows initiation of the numerical integration of Eq. (18) with $\delta=1$ and $\eta>0$.

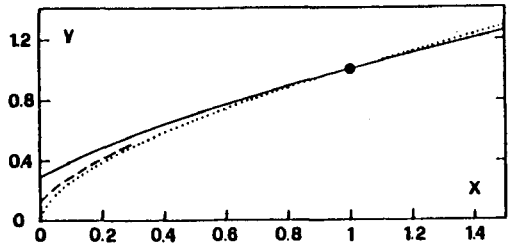

Fig. 2.
Non-dimensional free surface profile y(X) for (——) η=1, (---) η=0.5, (...) η=0 (kinematic wave approximation); (•) singular point.

For small η, $0<\eta<0.5$ say, Eq. (20) simplifies to

$$y_s' = \frac{3}{5}\left(1 - \frac{3\eta}{50}\right) \qquad (21)$$

Deviations between Eqs. (20) and (21) are then below 1%. For η=0, the slope of the free surface profile at the singular points is y_s'=3/5, while $y_s'(X=1, \delta=0)=0$.

Solutions of Eq. (18) obtained by numerical integration (Runge-Kutta method) are shown in Fig. 2 for typical values of η. Once the basic parameters p, K and S_o are prescribed, this diagram enables direct determination of the free surface profile.

Discussion of Results

The solution of Eq. (18) for $\eta>0$ and $\delta=1$ indicates that the effect of η on $y(X)$ becomes insignificant whenever $\eta<\eta_\ell$, in which η_ℓ is a limit number (Fig. 2). The solutions of Eq. (18) for $\eta>0$ and $\delta=1$ (dynamical relation) and the kinematic wave approximation $\eta=\delta=0$ then become nearly identical.

The numerical solution of Eq. (18) for small η and $\delta=1$ is not evident since its right hand side becomes a product of a large number ($1/\eta$) times an extremely small number ($1-X^2/y^{10/3}$). According to Morris and Woolhiser (1980) "the numerical technique for solution of the full de Saint Venant equations by the characteristic method ... breaks down for low values of F_o as well as for large k". The kinematic wave and the zero-inertia approaches are then the *only* possibilities to solve for the flow pattern. The exact solution for η=0 (kinematic wave approximation) is according to Eq. (18)

$$y = X^{3/5} \qquad (22)$$

In contrast, the zero-inertia flow model (δ=0) must be sought from

$$y' = \frac{1}{\eta}\left(1 - \frac{X^2}{y^{10/3}}\right) \qquad (23)$$

Fig. 3 compares the three different formulations, namely the surface profiles according to the dynamical, the zero-inertia and the kinematic wave approximations for (the extremely high value) η=1.

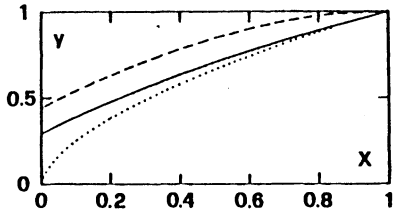

Fig. 3. Comparison of free surface profiles y(X) according to (——) dynamical, (---) zero-intertia, and (...) kinematic wave approximations for $\eta=1$.

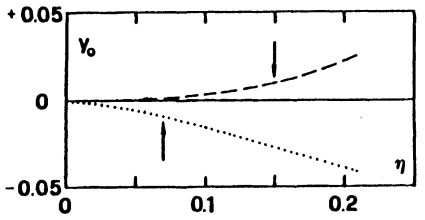

Fig. 4. Deviations of non-dimensional upstream flow depth according to(---) zero-intertia and (...) kinematic wave approximations when compared to (——) dymamical flow equation (18). Arrows indicate where deviations are 1%.

It is seen that the kinematic wave approach and the full dynamical relation fit well for relatively large distances X, $0.5 \leqslant X \leqslant 1$; however, slopes of the dynamical and the zero-inertia approach are nearly identical for small X. Consequently, the latter two fit better if the considered reach has finite length, $X<0.5$, and if the imposed boundary condition is identical for the two. It is interesting to note that $y(\delta=0)>y\ (\delta\neq 0)$, while $y(\eta=0)<y(\delta,\eta)$. The two approximations to the dynamical flow Eq. (18) are thus the upper and the lower bounds. The three formulations become identical for $\eta=0$ and may be considered as practical identical $\eta<\eta_\ell$. Consequently the kinematic wave approximation is an *asymptotical* solution of Eq. (18).

The flow depth at the upstream end of the plane, $y_o=y(X=0)$, can be considered as a degree of applicability of the dynamical and the zero-inertia wave approaches when compared to the respective flow depth $y_\eta=y(\eta=0)=0$ (kinematic wave approach). Based upon numerical integration of Eq. (18) with $\delta=1$ and $\delta=0$ Fig. 4 shows a plot of $y_o(\eta)$.

It is observed that the kinematic wave approximation deviates less than 1% from the upstream flow depth according to Eq. (18) for $\eta<\eta_\ell=0.07$, while $\eta_\ell=0.15$ for $\delta=0$ (zero-inertia approach). Inserting the first result (kinematic wave approach) into Eq. (19) then yields

$$p_{max} < \frac{0.07 \times g^2}{K^3 \sqrt{S_0}}, \tag{24}$$

Therefore, the *application criteria* of the kinematic wave approximation are

i) maximum *Froude number*, $\mathbf{F}_o$, be smaller than unity or, according to (Hager 1985) $\mathbf{F}_o^2=(K\sqrt{S_o})^{9/5}/g<1$, corresponding to $K\sqrt{S_o}<3$,

ii) shallowness of flow, $h_o/(S_oL)$ be very small, corresponding to Eq. (24) above.

In comparison the kinematic wave number (Woolhiser and Liggett 1967)

$$k = \frac{S_0 L}{h_0 F_0^2} > 10 \qquad (25)$$

is an *implicit* criterion for the applicability of the kinematic wave approach. It implies knowledge of the typical velocity, V_o, and the typical flow depth, h_o. The present approach allows specification of k using the two aforementioned criteria, i.e.

$$k = \frac{1}{\eta}\frac{1}{F_0^2} = \frac{g^2}{pK^3\sqrt{S_0}} \quad \frac{g}{(K\sqrt{S_0})^{9/5}} > \frac{1}{\eta_\ell} 1 \qquad (26)$$

Solving the right hand side for $p=p_{max}$ then yields

$$p_{max} < \frac{66}{(K^{24} S_0^7)^{1/5}} \qquad (27)$$

in which $K(m^{1/3}s^{-1})$. Consequently the kinematic wave approximation is a valid approach provided the roughness coefficient K is low, the bottom slope and the maximum excess precipitation are relatively small. As an exmple, assume $K=10$ $m^{1/3}/s$ ($n=0.10$), $S_o=0.1$ for which $p_{max}<0.026$ m/s in order that the kinematic and the dynamic wave approximations fit. Typical tropical excess precipitation has the order $p=100$ mm/h$= 2.8\times10^{-5}$ m/s which is much smaller than the above computed value. Consequently, the kinematic wave approximation is a valid approach for *arbitrary* overland flows.

However, the above criteria may become invalid for flows in small *streams* (collectors of overland flows in a watershed). Suppose, as an example, an excess precipitation $p=100$ mm/h on a sloping plane of length $x=1{,}000$ m and $S_o=0.1$.

For pseudo-steady flow conditions, the lateral inflow to the small stream characterised by $K=15$ $m^{1/3}/s$, $S_o=0.02$ and width $b=10$ m then is $p=q/b=0.1\times1{,}000/(3{,}600\times10)=0.0028$ m/s. The criterion regarding the Froude number, $K\sqrt{S_o}=15\sqrt{0.02}=2.12<3$, and $\eta=pK^3\sqrt{S_o}/g^2=0.014<0.07$ regarding the shallowness of the flow are fulfilled but near the respective limit values.

Conclusions

The present study compares often applied formulations of longitudinal momentum equations, namely the dynamical, the zero-inertia and the kinematic wave approximations for pseudo-steady flow conditions. It is found that

1) de Saint Venant's formulation (accounting for uniform velocity and hydrostatic pressure distribution) describes *shallow water* flows (neglect of streamline curvature effects).
2) The zero-inertia formulation may only be applied provided globally *subcritical* flow conditions prevail in addition.
3) The kinematic wave approximation, finally, holds only for thoroughly subcritical, *very shallow* flows.

4) Asymptotically, the three of the approaches become indentical. Application limits of the kinematic wave approximation are i) $K\sqrt{S_o}<3$ and ii) $pK^3\sqrt{S_o}/g^2<0.07$ on any subreach of a watershed. Condition i) deliminates dynamical effects (such as roll waves), while ii) excludes diffusive effects.
5) In practice overland flow is always governed by the kinematic wave approach, while flow in small streams has to be examined more carefully regarding the above (explicit) applicability criteria.

References

Borah, D.K., Prasad, S.N., and Alonso, C.V. (1980) Kinematic wave routing incorporating shock fitting, *Water Resources Research, Vol. 16*, 3, pp. 529-541.

Hager, W.H. (1981) Die Hydraulik von Verteilkanaelen, Thesis presented at the Swiss Federal Institute of Technology, ETH, Zürich, Vol. 6948, parts I & II, Zürich.

Hager, W.H. (1983) Open channel hydraulics of flows with increasing discharge, *J. Hydraulic Research, Vol. 21*, pp. 177-194.

Hager, W.H., and Hutter, K. (1984) Approximate treatment of plane channel flow, *Acta Mechanica, Vol. 51*, pp. 31-48.

Hager, W.H. (1985) Analysis of non-linear rainfall runoff process, *Nordic Hydrology, Vol. 16* (5).

Katopodes, N.D. (1982) On zero-inertia and kinematic waves, *Proc, ASCE, J. Hydraulic Engineering, Vol. 108, HY11*, pp. 1380-1387.

Liggett, J.A. (1975) Basic Equations of unsteady flows, in Unsteady flows in open channels, ed. by K. Mahmood and V. Yevjevich, Water Resources Publications, Fort Collins, Col.

Lighthill, M.J., and Whitham, G.B. (1955) On kinematic waves; I. Flood movement in long rivers, *Proc. Royal Society, Series A, London, Vol. 229*, pp. 281-316.

Morris, E.M., and Woolhiser, D.A. (1980) Unsteady one-dimensional flow over a plane: Partial Equilibrium and recession hydrographs, *Water Resources Research, Vol. 16, 2*, pp. 355-360.

Raudkivi, A.J. (1979) *Hydrology*, Pergamon Press, Oxford-New York.

Weinmann, P.E., and Laurenson, E.M. (1979) Approximate flood routing methods: a Review, *Proc. ASCE, J. Hydraulics Division, Vol. 105, HY12*, pp. 1521-1536.

Woolhiser, D.A., and Liggett, J.A. (1967) Unsteady, one-dimensional flow over a plane – the rising hydrograph, *Water Resources Research, Vol. 3*, pp. 753-771.

Woolhiser, D.A. (1975) Simulation of unsteady overland flow, in Unsteady flows in open channels, ed. by K. Mahmood and V. Yevjevich, Water Resources Publications, Fort Collins, Col.

Received: 4 July, 1985

Address:
Willi H. Hager,
École Polytechnique Fédérale de Lausanne,
Département de Génie Civil,
Institut de Travaux Hydrauliques,
CH-1015 Lausanne, Switzerland.

Kurt Hager,
Kuster & Hager,
Hydraulic and Wastewater Engineering,
Toenierstrasse,
CH-8730 Uznach, Switzerland.